

DETERMINATION OF DROPLET VELOCITY IN SQUARE MICROCHANNEL

JIN-YUAN QIAN^{1,2,3}, XIAO-JUAN LI¹, ZAN WU³, ZHEN CAO³ & BENGT SUNDEN³

¹ Institute of Process Equipment, College of Energy Engineering, Zhejiang University, PR China.

² State Key Laboratory of Fluid Power and Mechatronic Systems, Zhejiang University, PR China.

³ Department of Energy Sciences, Lund University, Sweden.

ABSTRACT

Generally, droplet velocity in liquid-liquid two-phase flow in microchannel is obtained via droplet displacement and time interval precise determination in sequential photos/videos. The precision is tightly related to shutter speed of the camera. In this paper, a novel method called direct image method is proposed to predict the droplet velocity. The droplet velocity can be easily obtained in one snapshot by this method. In order to validate the accuracy of this novel method, experiments are carried out in water-butanol, water-hexane and water-oil (Mogul Trafo CZ-A Paramo) systems. The droplet velocity predicted by this direct image method shows a good agreement with the experimental data. Although the assumptions which has been used to determine the droplet velocity still need to be improved, this method can be useful in industrial application.

Keywords: direct image method, droplet velocity, square microchannel.

1 INTRODUCTION

Microfluidic systems play an important role in industries such as chemical synthesis, solvent extraction and emulsion due to their superiority of high efficiency, low consumption, easy operation and controllable process [1]. Liquid-liquid two-phase flow system in micro-scale has a great significance in microfluidic systems. Common flow patterns in liquid-liquid two-phase flow systems are droplet flow, slug flow, deformed interface flow, jet flow and parallel flow [2]. Compared with other flow patterns, droplet flow is a more stable and preferred flow pattern because the droplet size and droplet formation frequency can be easily controlled. More importantly, the large surface-to-volume ratio and internal circulation inside the droplet can highly promote the mass transfer efficiency [3].

In liquid-liquid two-phase flow systems e.g. oil/water, the dispersed phase and the continuous phase are injected in microchannel, continuously. With the interaction of two phases, the dispersed phase is cut into small droplets. Many researches have been carried out to investigate the hydrodynamics of droplet flow in microchannel. Garstecki *et al.* [4] made detailed discussions to elaborate the forces involved in the droplet breakup process, which included the surface tension force, the shear stress force and the force arising from the increased resistance to flow of the continuous phase. Results showed that the pressure drop, which is from the high resistance, played a dominating role in the droplet breakup process. Characteristics of droplet flow such as droplet size and droplet formation frequency are mostly studied. Madadelahi *et al.* [5] proposed a fluidic barrier method to produce multiple droplets on a centrifugal microfluidic platform. Effect of rotational frequency on droplet size and uniformity of emulsions was investigated. Liu *et al.* [6] experimentally studied the dynamics of water-high-viscosity ionic liquid two-phase flow in a flow-focusing microchannel. Scaling laws for predicting the droplet volume and droplet formation frequency were proposed as a function of flow rate ratio

and capillary number of the continuous phase. In order to achieve production of homogeneous droplets, both experiments and simulations were carried out by Zhang *et al.* [7]. The droplet length and droplet formation frequency were measured at different capillary numbers and velocity ratios. Correlations based on the capillary number, total velocity and velocity ratio were proposed for predicting the droplet length and droplet formation frequency. Korczyk *et al.* [8] experimentally studied the dependence of droplet size on shear-capillary force ratio. Especially, leaking regime was detailed discussed. Models for predicting the droplet size and transition of flow patterns. Liquid properties also have a significant influence on the droplet size and droplet formation frequency. Yao *et al.* [9] experimentally studied the effect of liquid properties on the droplet formation process. Glycerol solutions and octane were selected as the liquid system. Both the influence of the continuous phase viscosity and the dispersed phase viscosity were considered. Results highlighted the effect of the continuous phase viscosity on droplet formation. Bai *et al.* [10] experimentally investigated the effect of the continuous phase viscosity on the droplet formation process. The continuous phase viscosity ranged from 0.5 to 1000 mPa s, which provided a wide range of the continuous phase viscosity. In addition, comprehensive experiments were carried out by Cao *et al.* [11] to investigate the hydrodynamics of droplet flow at different parameters, such as flow rate ratios, liquid properties and hydraulic diameter. A new correlation involving flow rate ratios, Weber number and Reynolds number was proposed for predicting the droplet length.

Furthermore, the droplet velocity is a very important parameter. It has a great impact on the overall transport time in microfluidic systems. In a microchannel with a specified channel length, a lower droplet velocity implies a higher residence time which means that molecules have sufficient time to transfer between phases. Plouffe *et al.* [12] investigated the flow regimes and mass transfer rates in five different micro-reactors. When conducting the experiments, two-phase alkaline hydrolysis of 4-nitrophenyl acetate was used. Flow regimes and convection of 4-nitrophenyl at different total flow rates were presented. Results showed that whether in a n-butanol/aqueous NaOH system or toluene/aqueous NaOH system, the variation of the conversion versus flow rate was similar. In droplet flow regime, an increase of the total flow rate led to a decrease of the conversion. This was attributed to the insufficient residence time. Besides, the droplet velocity is a key parameter concerning the droplet coalescence since the precise control of the droplet velocity is vital for the matching between two phases. Xu *et al.* [13] investigated droplet fuse using a railroad-like channel network. The droplet fuse efficiency was influenced greatly by the droplet velocity. Results indicated that when the droplet velocity was less than 9 mm/s, the two droplets were in contact a longer time. However, when the droplet velocity was greater than 11 mm/s, the contact time between the two droplets was too short so that they could not fuse efficiently.

Generally, the measured droplet velocity in a microchannel is always higher than the droplet superficial velocity, which is defined as sum of the continuous phase velocity and the dispersed phase velocity. Salim *et al.* [14] measured the droplet velocity in oil-water flow in a glass microchannel and compared them with the droplet superficial velocity. The droplet velocity was determined by the flow images recorded at intervals of 0.04 s. Results showed that the measured droplet velocity was approximately 1.28 times higher than the droplet superficial velocity. Yagodnitsyna *et al.* [15] measured the droplet velocity in kerosene-water, paraffin oil-water and paraffin oil-castor oil systems. Results showed that the measured droplet velocity in paraffin oil-castor oil was 1.81 times higher than the droplet superficial

velocity. However, the measured droplet velocity in paraffin oil-water was close to the droplet superficial velocity. This difference was attributed to the existence of the wall film between the droplet and the channel wall. Li *et al.* [16] measured the droplet velocity in microchannel with different diameters. Results showed that for the same droplet superficial velocity, the measured droplet velocity in the microchannel with a larger diameter was higher than that in the microchannel with a smaller diameter. In addition, the velocity profiles inside the droplet were analysed by micro-particle image velocimetry (μ PIV). For visualization, 3- μ m red dyed polystyrene microspheres were added in the dispersed phase. The droplet velocity obtained from the μ PIV and that determined by the plug displacement were compared.

Characteristics of droplet which include droplet length, droplet formation frequency and droplet velocity are very important parameters for a precise control of droplet flow in microchannel. Droplet length and droplet formation frequency are widely studied by many researchers. However, there are only few research works focussed on the droplet velocity in microchannel which affects the overall transport time in microfluidic systems. In this paper, a novel method for measurement of droplet velocity is proposed. Droplet velocity in water-butanol, water-hexane and water-oil (Mogul Trafo CZ-A Paramo) systems is determined using the direct image method and is compared with the droplet velocity estimated from sequential snapshots.

2 EXPERIMENTAL SETUP

2.1 Experimental apparatus

The test rig is shown in Fig. 1a. There are two high precision syringe pumps (New Era, NE-4000) for flow control of oil and water phases, a camera (Olympus OM-D E-M1) with a shutter speed of 1/30 s for capture of high-resolution pictures, a stereo microscope (Motic, SMZ-171) for flow visualization, a microchannel fabricated with borosilicate glass by Little Things Factory GmbH and a cold light source (Motic, MLC-150C) with two lighting arms for supply of brightness. Fig. 1b shows the dimensions of the microchannel. The microchannel is designed with a square cross section of 600 \times 600 μ m. It consists of two inlets for water injection and one inlet for oil injection. The outlet is exposed to atmosphere. The experiments were conducted at room temperature.

2.2 Materials

Three liquid-liquid two-phase systems are used for conducting the experiments. Aqueous phase is de-ionized water, and it is set as the continuous phase. Organic phases are butanol (Acros Organics, >> 99.5%), hexane (Acros Organics, >> 99.36%) and oil (Mogul Trafo CZ-A Paramo), respectively. Organic phase is set as the dispersed phase. The two-phase properties are listed in Table 1.

The interfacial tension values in three systems were measured by a drop volume tensiometer (Lauda TVT 2) with a measurement uncertainty of $\pm 5.0\%$. The viscosities of oil were measured by a DV-III Brookfield viscometer at room temperature with an uncertainty of $\pm 5.0\%$. In water-butanol and water-hexane systems, the liquids are injected in the microchannel at equal flow rates $Q_c = Q_d = 1.30\text{--}6.48$ ml/h. In water-oil system, the continuous phase flow rate and the dispersed phase flow rate are both in the range of 1.0–30.0 ml/h. The testing parameters are listed in Table 2.

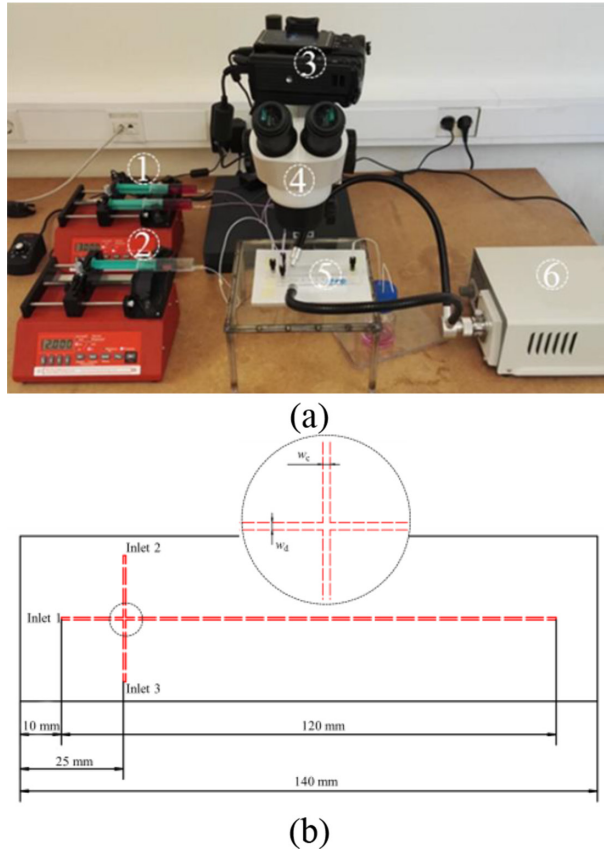


Figure 1: Test rig for conducting the experiment. (a) Experimental apparatus: 1. syringe pump for water injection; 2. syringe pump for oil injection; 3. camera; 4. microscope; 5. microchannel; 6. cold light source. (b) Dimensions of the microchannel.

3 THE DIRECT IMAGE METHOD FOR DETERMINING DROPLET VELOCITY

Generally, in order to estimate the droplet velocity, a high-speed camera is used to capture the sequential photos/videos. Then, the video is switched with real small time steps. With the distance in two photos and the time step, the droplet velocity can be determined [12, 17]. This process needs a relatively high requirement for resolution of camera, and a very careful capture is needed during the post-process of the experimental data. Mohammed *et al.* [18] proposed an image processing technique which involved approximate medina method and blob extraction analysis for the measurements of transitional slug velocity and slug length. However, this kind of method also relies on the image motion tracking steps.

Here, a novel method is proposed for determining the droplet velocity. As shown in Fig. 2, the dispersed phase is injected into microchannel with a constant flow rate of Q_d . With the interaction of the dispersed phase and the continuous phase, the droplet is produced in a specified time interval Δt . The droplet volume V can be determined by eqn (1).

$$V = Q_d \Delta t \tag{1}$$

Meanwhile, in the specified time interval Δt , the previous droplet flows a distance Δd , where

Table 1: Two-phase properties used in experiments.

Materials	Phase role	Physical properties		
		ρ (kg/m ³)	μ (mPa·s)	σ (mN/m)
Water	Continuous phase	998.2	1	–
Butanol	Dispersed phase	810	2.94	1.8
Hexane	Dispersed phase	654.8	0.3	51
Oil	Dispersed phase	826	14.5	45.5

$$\Delta d = u\Delta t \quad (2)$$

In eqn (2), u represents the droplet velocity in microchannel. Based on eqns (1) and (2), the real velocity of the droplet flow can be derived as shown in eqn (3).

$$u = \Delta d \frac{Q_d}{V} \quad (3)$$

In eqn (3), Q_d is set by the user, and Δd and V can be obtained in one picture. Therefore, the droplet velocity can be easily obtained. Using the novel method, there is only one picture needed. It should be noted that Δd is the average value based on measurements in five snapshots. The maximum relative error is 4%.

4 MEASUREMENT OF DROPLET CHARACTERISTICS

4.1 Film thickness

Considering the wetting behaviour between the phases and walls, two possibilities exist: the droplet is either surrounded by a thin film of the continuous phase or without a film [19]. The existence of the thin film facilitates the droplet flow in microchannel. It makes the droplet to move at a higher velocity than the mixture superficial velocity [15]. Ghaini *et al.* [20] investigated the film thickness at several known droplet velocities in a water-kerosene system. The film thickness was obtained by processing the fluorescence intensity signal at the centre of the capillary. Results indicated that the film thickness was increased with an increase of droplet velocity, but when the droplet velocity was higher than 100 mm/s, the film thickness was kept constant. In the present experiments, the photos reveal that the continuous thin film always existed in all experiments although the film thickness was related to the working conditions. Due to the extremely thin wall film, the measurement of film thickness becomes very difficult from the experimental snapshots. Thus, the film thickness is predicted based on the

Table 2: Testing parameters in three different systems.

Liquid-liquid two-phase systems	$Ca_c (\times 10^{-5})$	$Ca_d (\times 10^{-5})$	$\Phi (Q_d/Q_c)$
Water-butanol	55–280	160–820	0.5
Water-hexane	1.9–9.8	0.58–3	0.5
Water-oil	0.85–51	24–740	0.05–1

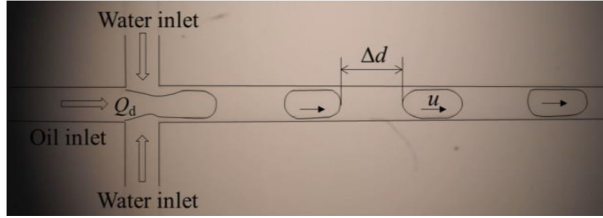


Figure 2: Illustrations for predicting the droplet velocity in microchannel: snapshot recorded by camera.

scaling law, which was presented by Yao *et al.* [21]. When $Ca_d < 0.01$, the film thickness can be predicted by the scaling law proposed by Fairbrother and Stubbs [22], see eqn (4).

$$\delta = 0.5RCa_d^{0.5} \tag{4}$$

$$Ca_d = \frac{\mu_d u_d}{\sigma} \tag{5}$$

where δ represents the film thickness, R represents the radius of the droplet cap and Ca_d is the capillary number of the dispersed phase. Figure 3 shows the characteristics of droplet flow in different systems.

It can be seen that the droplet contacts the channel wall very closely and the droplet cap is nearly hemispherical. An assumption is made that the radius of the droplet cap is considered as half of the channel width i.e. $R = w/2$. Therefore, the film thickness for each condition can be predicted. According to eqns (4) and (5), the film thickness is affected by not only the radius of the droplet cap but also the fluid properties. Figure 4 presents the correlation between the film thickness and the capillary number of the dispersed phase. It should be noted that the film thickness in a water-hexane system is remarkably low. This is attributed to the extremely low ratio of the viscosity to the surface tension.

4.2 Droplet velocity

In this section, the droplet velocity at different conditions are predicted using the direct image method. The predicted droplet velocity is compared with the droplet velocity which was determined via the sequential photos.

As mentioned in Section 4.1, in the present experiments, the photos reveal that a continuous thin film always exists in all the experiments. The existing film thickness facilitates the droplet flow in the microchannel at a higher velocity. Figure 5 depicts the correlation between the droplet superficial velocity and the droplet real velocity measured via the sequential photos. It can be seen that the droplet flows in the microchannel at a higher velocity than the droplet superficial velocity undoubtedly.

Actually, when the droplet velocity is predicted by eqn (3), biggest challenge is how to calculate the droplet volume precisely. The simplification of the droplet shape is crucial for accurate predictions. Based on discussion in section 4.1, here, the droplet shape can be assumed as a combination of a cube and two hemispheres. Figure 6 illustrates the schematic diagram for the droplet volume determination.

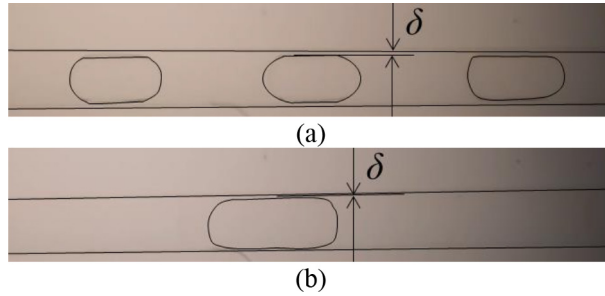


Figure 3: Characteristics of droplet flow in different systems. (a) Water-butanol system, $Q_c = Q_d = 1.3$ ml/h; (b) water-hexane system, $Q_c = Q_d = 1.3$ ml/h.

In Fig. 6, L represents droplet length, and δ , R and w represent the film thickness, radius of the droplet cap and microchannel width, respectively. The droplet lengths at different conditions are measured, and the dimensionless droplet length at different droplet superficial velocities is plotted in Fig. 7. The droplet length for each condition is measured with uncertainties of $\pm 5\%$, $\pm 8\%$ and $\pm 5\%$ in water-butanol system, water-hexane system and water-oil system (Mogul Trafo CZ-A Paramo), respectively. In addition, it can be seen from Fig. 4 that the maximum radius of the droplet cap only accounts for 4.5% of the radius of the microchannel. Therefore, the droplet volume can be predicted by eqn (6), where $R = w/2$. Equation (6) is also adopted by Di Miceli Raimondi *et al.* [23] for calculation of the droplet volume.

$$V = \frac{4}{3}\pi R^3 + (L - 2R)(2R)^2 \quad (6)$$

In order to validate the accuracy of eqn (6), the droplet volume predicted by eqn (6) and determined by the experiment is compared, as shown in Fig. 8. The x-axis and y-axis represent the results determined in experiment and eqn (6), respectively.

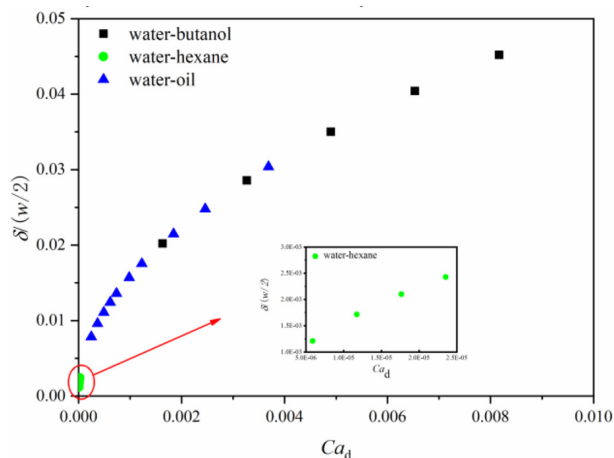


Figure 4: Correlation between the film thickness and the capillary number of the dispersed phase.

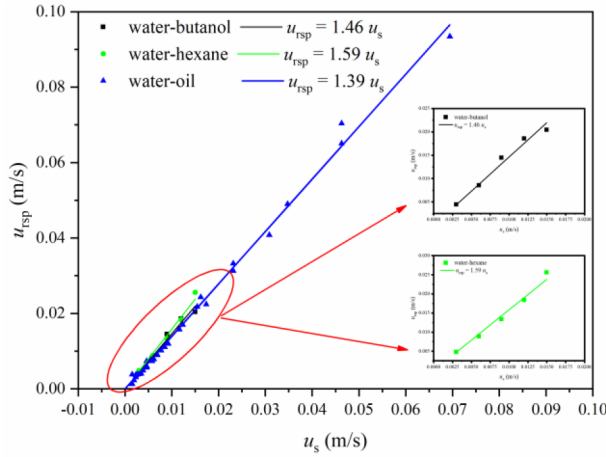


Figure 5: Droplet superficial velocity versus droplet velocity measured via the sequential photos in three different systems.

The droplet volume determined by the experiment is determined by eqn (1). Figure 8 shows good agreement between the predicted droplet volume and the determined droplet volume by the experiments. The relative error is less than 10%. Therefore, based on eqns (3) and (6), the droplet velocity can be predicted precisely. Figure 9 presents the predicted droplet velocity versus droplet real velocity determined by the sequential snapshots. It shows a good agreement between the two velocities. Thus, it can be concluded that the proposed method can be used for determining the droplet velocity accurately.

4.3 Limitations

Based on above discussions, the droplet velocity can be directly estimated via this new method. However, limitations still exist.

The film thickness is a key factor to determine the droplet volume. In this paper, it is roughly estimated by considering the radius of the droplet cap as half of the channel width. Later, the determination of the film thickness should be further improved.

The proposed method is incapable to calculating the velocity of droplet which formed with a low frequency since the distance the adjacent droplets may be larger than the frame size.

5 CONCLUSIONS

In this paper, a novel method for determining the droplet velocity is proposed, and experiments are carried out to testify the accuracy of the new method. Remarkable conclusions are made as follows: three liquid-liquid two-phase systems are selected to produce droplet

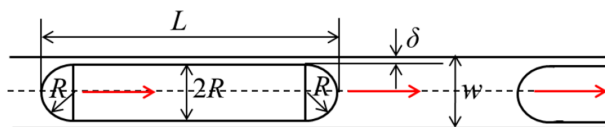


Figure 6: Schematic diagram for droplet volume determination.

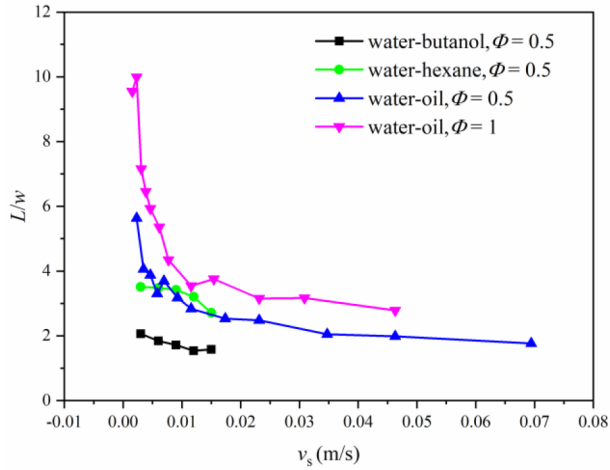


Figure 7: The dimensionless droplet length at different droplet superficial velocities.

flow in microchannel. The droplets formed in the experiments are all surrounded by a thin film. The existence of the thin film makes the droplet flow in microchannel to have a velocity higher than the mixture superficial velocity. The droplet velocity predicted by the novel method is compared with the experimental data. A good agreement is achieved. Although the measurement uncertainties existed, the proposed method provides an easier approach to estimate the droplet velocity. It should be noted that, when predicting the droplet real velocity via this method, precise measurements of the droplet length and droplet flow distance are necessary. In addition, the droplet shape should be assumed reasonably accurate according to the snapshots.

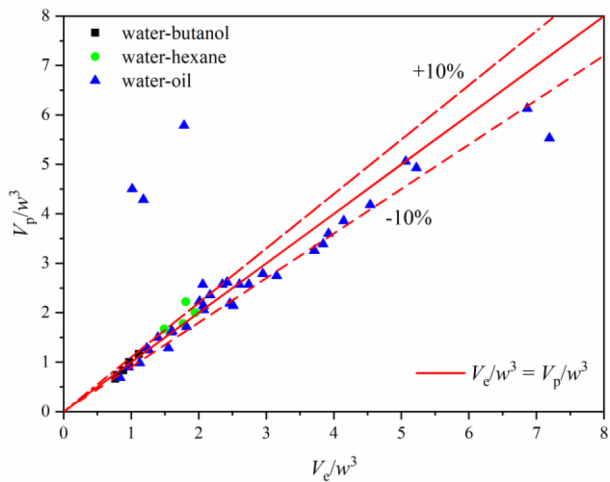


Figure 8: Comparisons of the droplet volume between the predicted one and determined by the experiment.

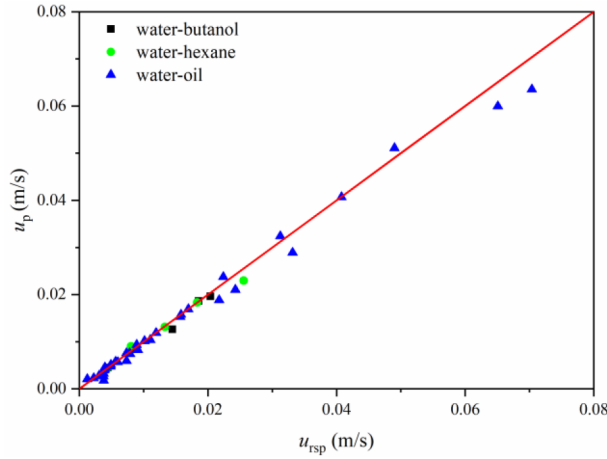


Figure 9: Comparisons of the droplet velocity between the predicted one and determined by the experiment via the sequential photos.

ACKNOWLEDGEMENTS

This work is supported by the National Natural Science Foundation of China (NSFC) through grant no. 51805470. This work is also financially supported by the Swedish Research Council.

NOMENCLATURE

Ca	Capillary number	<i>Greek symbols</i>	
L	droplet length, μm	μ	viscosity, $\text{mPa}\cdot\text{s}$
σ	interfacial tension, mN/m	ρ	density, kg/m^3
Q_c	continuous phase flow rate, ml/h	δ	film thickness, μm
Q_d	dispersed phase flow rate, ml/h	σ	interfacial tension, mN/m
R	radius of the droplet cap, μm	Φ	flow rate ratio of the dispersed phase to the continuous phase
u_p	droplet velocity predicted by the proposed method, m/s	<i>subscript</i>	
u_{rsp}	droplet real velocity measured via sequential photos, m/s	c	continuous phase
u_s	droplet superficial velocity, m/s	d	dispersed phase
V	droplet volume, μm^3	e	experimental
w_c	continuous phase channel width, μm	p	predicted
w_d	dispersed phase channel width, μm	s	superficial
Δd	droplet flow distance, μm	rsp	real, sequential photos
Δt	time interval, s		

REFERENCES

- [1] Wang, K. & Luo, G., Microflow extraction: A review of recent development. *Chemical Engineering Science*, **169**, pp. 18–33, 2017. Wang, K. & Luo, G., Microflow extraction: A review of recent development. *Chemical Engineering Science*, **169**, pp. 18–33, 2017. <https://doi.org/10.1016/j.ces.2016.10.025>
- [2] Qian, J., Li, X., Wu, Z., Jin, Z. & Sunden, B., A comprehensive review on liquid–liquid two-phase flow in microchannel: flow pattern and mass transfer. *Microfluidics and Nanofluidics*, **23(10)**, 2019. <https://doi.org/10.1007/s10404-019-2280-4>
- [3] Yao, C., Zhao, Y., Ma, H., et al., Two-phase flow and mass transfer in microchannels: A review from local mechanism to global models. *Chemical Engineering Science*, **229**, p. 116017, 2021. <https://doi.org/10.1016/j.ces.2020.116017>
- [4] Garstecki, P., Fuerstman, M.J., Stone, H.A. & Whitesides, G.M., Formation of droplets and bubbles in a microfluidic T-junction—scaling and mechanism of break-up. *Lab on a Chip*, **6(3)**, p. 437, 2006. <https://doi.org/10.1039/b510841a>
- [5] Madadelahi, M., Madou, M.J., Nokoorani, Y.D., et al., Fluidic barriers in droplet-based centrifugal microfluidics: Generation of multiple emulsions and microspheres. *Sensors and Actuators B: Chemical*, **311**, p. 127833, 2020. <https://doi.org/10.1016/j.snb.2020.127833>
- [6] Liu, C., Zhang, Q., Zhu, C., Fu, T., Ma, Y. & Li, H.Z., Formation of droplet and “string of sausages” for water-ionic liquid ([BMIM][PF6]) two-phase flow in a flow-focusing device. *Chemical Engineering and Processing - Process Intensification*, **125**, pp. 8–17, 2018. <https://doi.org/10.1016/j.cep.2017.12.017>
- [7] Zhang, S., Guivier-Curien, C., Veessler, S. & Candoni, N., Prediction of sizes and frequencies of nanoliter-sized droplets in cylindrical T-junction microfluidics. *Chemical Engineering Science*, **138**, pp. 128–139, 2015. <https://doi.org/10.1016/j.ces.2015.07.046>
- [8] Korczyk, P.M., van Steijn, V., Blonski, S., et al., Accounting for corner flow unifies the understanding of droplet formation in microfluidic channels. *Nature Communications*, **10**, p. 2528, 2019. <https://doi.org/10.1038/s41467-019-10505-5>
- [9] Yao, C., Liu, Y., Xu, C., Zhao, S. & Chen, G., Formation of liquid–liquid slug flow in a microfluidic T-junction: Effects of fluid properties and leakage flow. *AIChE Journal*, **64(1)**, pp. 346–357, 2018. <https://doi.org/10.1002/aic.15889>
- [10] Bai, L., Fu, Y., Zhao, S. & Cheng, Y., Droplet formation in a microfluidic T-junction involving highly viscous fluid systems. *Chemical Engineering Science*, **145**, pp. 141–148, 2016. <https://doi.org/10.1016/j.ces.2016.02.013>
- [11] Cao, Z., Wu, Z. & Sundén, B., Dimensionless analysis on liquid–liquid flow patterns and scaling law on slug hydrodynamics in cross-junction microchannels. *Chemical Engineering Journal*, **344**, pp. 604–615, 2018. <https://doi.org/10.1016/j.cej.2018.03.119>
- [12] Plouffe, P., Roberge, D.M. & Macchi, A., Liquid–liquid flow regimes and mass transfer in various micro-reactors. *Chemical Engineering Journal*, **300**, pp. 9–19, 2016. <https://doi.org/10.1016/j.cej.2016.04.072>
- [13] Xu, L., Lee, H., Panchapakesan, R. & Oh, K.W., Fusion and sorting of two parallel trains of droplets using a railroad-like channel network and guiding tracks. *Lab on a Chip*, **12(20)**, p. 3936, 2012. <https://doi.org/10.1039/c2lc40456g>
- [14] Salim, A., Fourar, M., Pironon, J. & Sausse, J., Oil-water two-phase flow in microchannels: Flow patterns and pressure drop measurements. *The Canadian Journal of Chemical Engineering*, **86(6)**, pp. 978–988, 2008. <https://doi.org/10.1002/cjce.20108>

- [15] Yagodnitsyna, A.A., Kovalev, A.V. & Bilsky, A.V., Flow patterns of immiscible liquid-liquid flow in a rectangular microchannel with T-junction. *Chemical Engineering Journal*, **303**, pp. 547–554, 2016. <https://doi.org/10.1016/j.cej.2016.06.023>
- [16] Li, Q. & Angeli, P., Experimental and numerical hydrodynamic studies of ionic liquid-aqueous plug flow in small channels. *Chemical Engineering Journal*, **328**, pp. 717–736, 2017. <https://doi.org/10.1016/j.cej.2017.07.037>
- [17] Ma, R., Zhang, Q., Fu, T., Zhu, C., Wang, K., Ma, Y. & Luo, G., Manipulation of microdroplets at a T-junction: Coalescence and scaling law. *Journal of Industrial and Engineering Chemistry*, **65**, pp. 272–279, 2018. <https://doi.org/10.1016/j.jiec.2018.04.038>
- [18] Mohammed, A.O., Nasif, M.S., Al-Kayiem, H.H. & Time, R.W., Measurements of translational slug velocity and slug length using an image processing technique. *Flow Measurement and Instrumentation*, **50**, pp. 112–120, 2016. <https://doi.org/10.1016/j.flowmeasinst.2016.06.016>
- [19] Kashid, M.N., Renken, A. & Kiwi-Minsker, L., CFD modelling of liquid–liquid multiphase microstructured reactor: Slug flow generation. *Chemical Engineering Research & Design*, **88(3)**, pp. 362–368, 2010. <https://doi.org/10.1016/j.chemd.2009.11.017>
- [20] Ghaini, A., Mescher, A. & Agar, D.W., Hydrodynamic studies of liquid–liquid slug flows in circular microchannels. *Chemical Engineering Science*, **66(6)**, 1168–1178, 2011. <https://doi.org/10.1016/j.ces.2010.12.033>
- [21] Yao, C., Zhao, Y. & Chen, G., Multiphase processes with ionic liquids in microreactors: Hydrodynamics, mass transfer and applications. *Chemical Engineering Science*, **189**, pp. 340–359, 2018. <https://doi.org/10.1016/j.ces.2018.06.007>
- [22] Fairbrother, F. & Stubbs, A., Studies in electro-endosmosis Part VI The “bubble tube” method of measurement. *Journal of the Chemical Society*, pp. 527–529, 1935. <https://doi.org/10.1039/jr9350000527>
- [23] Di Miceli Raimondi, N., Prat, L., Gourdon, C. & Tasselli, J., Experiments of mass transfer with liquid–liquid slug flow in square microchannels. *Chemical Engineering Science*, **105**, pp. 169–178, 2014. <https://doi.org/10.1016/j.ces.2013.11.009>